Turning Mechanisms for Airborne LiDAR and Photographic Data Acquisition

Article *in* Journal of Applied Remote Sensing · November 2013

DOI: 10.1117/1.JRS.7.073488

1 author:

Ajay Dashora
Indian Institute of Technology Guwahati
8 PUBLICATIONS **71** CITATIONS

SEE PROFILE

Journal of
Applied Remote Sensing

Turning mechanisms for airborne LiDAR and photographic data acquisition

Ajay Dashora
Bharat Lohani

SPIE

Turning mechanisms for airborne LiDAR and photographic data acquisition

Ajay Dashora and Bharat Lohani
Indian Institute of Technology Kanpur, Department of Civil Engineering, Kanpur 208016, India
ajayd@iitk.ac.in, ajaydashora@gmail.com

Abstract. Flight duration, which consists of strip time and turning time, is an important element of flight planning of airborne surveys as it affects the cost of data acquisition. The turning time dominates over the strip time and thus dictates the flight duration. However, the current practices of flight planning assume it as a constant for easier calculations in flight planning. Further, there is no literature available explicitly on turning mechanisms for airborne surveys. Instead of assuming a constant or following the complicated models of turning, this paper advocates simple heuristic-based models and turning mechanisms. The models and turning mechanisms are developed by considering the feasibility of flight operations, experiences of pilots, and the available approximate models of turning in the literature. The paper illustrates consecutive and nonconsecutive turning mechanisms and derives comprehensive mathematical formulations to represent these. An algorithmic scheme for selection of an optimal turning mechanism is presented. The paper argues that the discussed turning mechanisms and algorithms can be combined with the strip time for arriving at the optimal flight plan using the genetic and evolutionary algorithms. The developed approach can be easily incorporated into the present knowledge base of flight planning. [DOI: 10.1117/1.JRS.7.073488]

Keywords: turning mechanism; turning time; consecutive turning; nonconsecutive turning; flight duration.

Paper 13116 received Apr. 12, 2013; revised manuscript received Sep. 25, 2013; accepted for publication Oct. 3, 2013; published online Nov. 5, 2013.

1 Introduction

Airborne LiDAR and photographic data are acquired by integrating respective sensors with global positioning system (GPS) and inertial measurement unit (IMU), and mounting these in an aerial platform (aircraft or helicopter). The aerial platform flies over the ground with minimum variations in altitude and attitude. In general, the information of the ground is collected by forming rectangular strips of fixed swath, which are controlled by the sensor's field of view (FOV) and the flying height. The center line of the rectangular flight strip on a map is the two-dimensional projection of the flight line. The width of swath and overlap between adjacent flight strips decide the effective swath, which is equal to the swath minus overlap at a specific terrain elevation (or datum) and the number of flight lines. Therefore, effective swath is used to calculate the number of parallel flight strips (and flight lines) required to cover a given area of interest (AOI).[1] After collecting the data on a flight strip, an aerial platform navigates to the next flight line by taking a turn. Therefore, the flight duration or air time of aerial survey over the AOI essentially consists of the time to cover the flight strips (strip time) and turning between the flight strips (turning time). The periodic turning not only allows for the switching between the flight strips but also avoids the inaccuracies in heading angle measurement by IMU.[2] The process of flying over the strip and turning continues till data collection is completed or the endurance limit of the aerial platform is reached.

According to the type of the aerial platform, turning is practically performed by turning on the consecutive or nonconsecutive flight strips. Turning from a flight strip to the consecutive flight strip is called consecutive turning. However, with fixed wing aircrafts, which are not

0091-3286/2013/$25.00

suitable for sharp turns by employing steep bank angle, it is economic to turn with shallow bank angle and larger radius of turn to a nonconsecutive flight strip.[3] Air Traffic Bulletin[4] addresses the turnings with consecutive and nonconsecutive manners as the line coverage and block coverage, respectively.

The cost of the airborne data is higher than space-borne data due to the use of manned aerial vehicle and fuel consumption. Moreover, for airborne LiDAR, the acquisition cost per point is highest.[5] As a result, the cost of LiDAR and photogrammetry data is highly dictated by the duration of the flight, which is inversely proportional to the effective swath of the flight strip and the cruise speed of the aerial platform. The swath and speed of the aerial platform are decided according to the various data requirements (e.g., data density, spacing, etc.) and other constraints. Increasing either the flying height or the FOV increases the effective swath, which in turn reduces the number of flight strips for a given AOI and results in smaller flight duration. Furthermore, aligning the flight strips along the longest direction of an AOI leads to minimization of the number of flight strips for a given swath width and reduces the cost of data acquisition.[6]

Increasing the cruise speed reduces the strip time, though it causes an increase in the turning time. This is due to the fact that the turning time on a circular trajectory is proportional to the cruise speed.[7] On the other hand, as the time required to perform a turn is inversely proportional to the banking angle, it is obvious that a higher banking angle is desired.[8] However, the maximum bank angle is dictated by the stall speed of an aerial platform,[8,9] GPS lock, and the comfort of flying crew as repetitive air operations like maneuvering with steep banking angle may cause fatigue and airsickness.[10,11] On the contrary, with a small banking angle, spending more time in air is not desired as the aircraft would be exposed to more disturbances and the flying crew may lose concentration due to fatigue caused by prolonged flight duration.[11] Although a maximum banking of 45 deg is possible with GPS-assisted surveys, the flight planners limit the maximum banking angle to 25 deg for fixed-wing aircrafts, due to the reasons discussed above.[3,12]

Apart from the physical limitations of flying and the comfort of the flying crew, it is required to maintain a high precision during a turn in order to meet the next flight strip at the desired point. However, to account for the possibility of misalignment during turning, a point that is situated on the next flight line at a distance, which is equivalent to specified time buffer from the end of the next flight line, is approached by the pilot. This buffer time, which is addressed in this paper as "cushion period," provides sufficient time or cushion for conforming to the correct flying parameters (zero bank angle, flying height, speed, flying direction) and possible course correction before reaching the starting point of the upcoming flight line.[3] Further, it also provides enough opportunity for a pilot to ensure the desired operational needs with comfortable navigation. Fixed-wing aircraft, unlike a helicopter, is not appropriate for sharp turns with steep bank angles and demands a cushion period ranging from 30 to 60 s. However, a helicopter can perform sharp turns and is easier to align, requiring only 15 s as a cushion period.[3]

For a given cruise speed of aerial platform, irrespective of the length of the flight strip, the turning time between the flight lines is independent of strip time. However, turning time and strip time cannot be separated for decision making in the flight planning process as the data requirements and other constraints are the functions of variables involved in both strip time and turning time. For example, the data density of airborne LiDAR is a function of both swath width and cruise speed.[1] Further, for most of the flight planning missions, it is observed that the turning time is considerably higher than the strip time.[11] A simple calculation can explain that for a 2-km long strip, an aerial platform at a cruise speed of 50 m/s requires 40 s to fly over it. On the contrary, the text book on "Flight planning of aerial photography for mapping" by Read and Graham[11] and the online document titled "Guidelines of airborne LiDAR data acquisition" by Piel and Populus[13] suggest 3 to 4 min duration as an estimate of time required per turn between two adjacent and parallel flight lines for GPS- and IMU-assisted airborne surveys. According to private communication with Dr. Gary Llewellyn[12] of Natural Environment Research Council (NERC) Airborne Survey and Research Facility (Oxford, UK) and Dr. Jacques Populus[14] of Department of Coastal Environment Dynamics (Applications Géomatiques, Plouzane, France), the value of turning time for each turn is considered in the range of 2.5 to 5 min. Therefore, due to the apparently higher value of turning time than strip time, the turning time plays an important role in flight planning of an aerial survey. Consequently, when minimizing the flight duration to reduce mission cost, the turning time cannot be ignored or considered as a constant.

The current practice of flight planning calculates the strip time by estimating the sum of the times needed to cover flight strips in the predefined flying direction on an AOI. However, in the absence of any precise mathematically calculated value of turning time, as stated earlier, it is common practice to assume it is a constant. The constant time of turning per turn is adopted according to experience of flight planners and available heuristic information. The commercial software for flight planning either have an in-built constant value of turning time per turn or demands it as a user input. Moreover, the software tools do not have any provision for decision making by modeling different turning mechanisms.

The constant turning time including cushion period facilitates the decision-making process with less computational load. As a result, a semiautomatic approach, which involves the use of software tools and manual intervention, in decision making for the flight planning is used, which, however, is not efficient and accurate. On the other hand, mathematical modeling for switching between the parallel flight strips in consecutive or nonconsecutive manner for covering entire AOI in the minimum time is equivalent to the problem of traveling on parallel edges and shifting from one edge to the other in minimum time. The problem of traveling on parallel edges and switching between these is nonsolvable in polynomial time using classical combinatorial optimization techniques.[15] However, genetic algorithms (GA) and evolutionary algorithms (EA), which are based on rigorous search process and require minimal manual intervention, can be used for solving this optimization problem when the classical methods are less efficient or nonapplicable. For example, Rodrigues and Ferreira[16] combined the GA and local search method for solving the shortest path of travel on edges (or rural postman problems). Believing that GA (or EA) with or without classical optimization methods can solve this problem satisfactorily, this paper attempts to explain the turning mechanisms that are practiced in field for airborne surveys but not available explicitly in the literature so as to include these in a flight optimization system. The paper first explains the types of turning mechanisms with the terminology employed. Later, the designs of the turning mechanisms with their mathematical expressions are presented. Further, an algorithm scheme for decision making, which calculates the time of turning for different turning mechanisms and selects the optimal turning mechanism for the given cruise speed, banking angle, and cushion period, is suggested. In addition, some calculations, which conform to the thumb rules and heuristic information, are also demonstrated.

2 Terminology

Consecutive and nonconsecutive types of turnings are represented by the order of flight strips flown. Information of the turn is conveyed by augmenting the direction of flight path over the flight line with ordering of the flight lines (or flight strips). Generally, the order of flight lines being covered is given using the direction of flight in these strips and the flight strip number. The flight direction of a flight path can be fore (F) or rear (R). The flight direction is fore if the flight is being carried out in the same direction as that of the direction of flight on the first flight line. A flight in the opposite direction to the fore direction is called rear. A combination of flight lines and flight directions can be shown as 1F-2R-3F-4R, which represents the order of flight strips being covered and their direction of coverage. This further represents that between two flight lines, a turn is being taken, which is the consecutive turn in this case as the successive flight lines are being covered with the progress of flight. A turn can also be called clockwise or anticlockwise depending on how an aircraft is taking a turn when seen from zenith. In case of a nonconsecutive turn (NCT), the flight numbers will not occur in monotonically increasing order but will change, e.g., 1F-6R-2F-7R-3F-8R-4F-9R-5F-10R. The naming convention for nonconsecutive turning is explained in detail in the relevant section of this paper.

It is evident that in either of the turning types, the aircraft alters the direction of flight from one particular flight line to the next flight line till survey operations are completed. The duration of a turn is modeled for consecutive and nonconsecutive turning in the following sections. Moreover, in general, flying operations are avoided or not performed in the presence of winds.[3] However, under compelling circumstances, flying operations at the cost of additional expenses are performed under the presence of winds if the wind speed is <20 knots (10.3 m/s).[3,13] In this paper, the wind speed is assumed as zero and thus not considered in time calculations.

The turning is performed in horizontal plane at a given flying height with a cruise speed that is equal to the true air speed of the aerial platform. Therefore, turns are level turns. In the forthcoming discussion, aerial platform and cruise speed (V) are, respectively, addressed as "aircraft" and "speed."

3 Modeling of Consecutive Turns

The separation between the consecutive flight lines is equal to the effective swath (B), which is actual swath minus the overlap between flight strips. There are three possible cases of the relative sizes of the values of effective swath (B) and the required turning width (h_t), viz., effective swath (B) is more than, less than, or equal to the required turning width (h_t) of a 180-deg level turn (also called horizontal course reversal). Read and Graham[11] and Graham and Koh[17] mention the simple geometric arrangement of direct turn, U turn, and S turn. Read and Graham[11] further suggest 30/30 procedure turn, which is a modification over S turn, for consecutive turning in GPS-assisted aerial surveys. The characteristic design of all these turns utilize the available space or create an adequate space for a 180-deg level turn with a given speed of aircraft and bank angle. When the effective swath is less than the width of half circular turn ($B < h_t$), it requires a change in the direction of flight (or heading) such that it creates a space for a 180-deg level turn (Fig. 1). In this case, the consecutive turns are formulated appropriately by modifying 30/30 turn and S turn for varying locations of the ends of the consecutive flight lines. Conversely, an effective swath value more than or equal to the diameter (or width h_t) allows an aircraft to switch to consecutive flight line by U turn, which is formed by two quarter turns separated by straight horizontal flight line segment. Depending on the value of the swath, the length of the horizontal line segment varies from zero to a finite value.

The mathematical formulations for all three cases, which combine and modify the 30/30 procedure turn, direct turn, and U turn as per the aviation practices commonly adopted by pilots in field, are presented below to calculate the total turn time (T_T). Figure 1 shows the two adjacent flight strips by rectangular boxes and respective flight lines by dotted lines. Moreover, turning is shown between the right ends of two flight lines. The following symbols are used in formulations and figures:

$i = i$'th flight line
$i + 1 = (i + 1)$'th flight line
$X_i^L = X$ coordinate of left end of the i'th flight line
$X_{i+1}^L = X$ coordinate of left end of the $(i + 1)$'th flight line
$X_i^R = X$ coordinate of right end of the i'th flight line
$X_{i+1}^R = X$ coordinate of right end of the $(i + 1)$'th flight line
ψ = Change in the heading angle of aircraft at the end of i'th flight line
ψ_{Max} = Maximum allowable change in the heading angle of aircraft (user input)

Case-1 ($B < h_t$): Figure 1 depicts the schematic view of consecutive turning by 30/30 turn, which consists of inclined linear path and circular path. The turning process starts at the end of the upper flight line at point A. From point A to C, the aircraft changes the heading angle by ψ. At point C, the aircraft starts to follow a circular trajectory and performs a horizontal course reversal (or 180-deg level turn) and reaches the subsequent flight line at point D. During

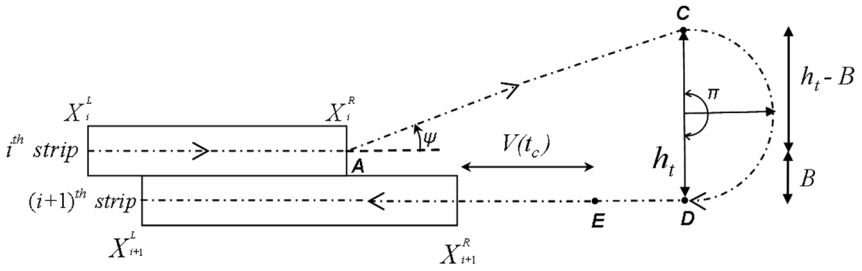

Fig. 1 Schematic view of two consecutive flight lines and flight path with cushion period in a consecutive turn.

turning, the change in the heading angle is realized by following a combination of transition curves and an arc of a circle. Consequently, in addition to the straight line and circular curve, the length of the flying path (travel length) is also made of the transition curves that provide a smooth change in the bank angle and the direction of flight. In addition to this, the relative positions (X coordinates) of the ends of two adjacent flight lines also dictate the length of the travel (as shown in Fig. 2).

The complete geometric arrangement including the transition curves from point A to point C can be modeled by different geometric methods and curves. Conventionally, transition curve in level turn is modeled by Cornu spiral or Euler spiral, which is a clothoid curve.[18,19] The solutions proposed by Dai and Cochran,[18] Techy et al.,[19] and others (e.g., McCrae[20]) are complicated and iterative due to the involvement of Fresnel integral in mathematical expressions. On the other hand, a pilot performs a turn according to his/her personal comfort. A naturally comfortable agreement is to adhere to flat turns. Flat turn means a level turn with a very large radius of curvature, which appears very close to a straight line over a short length of the trajectory. A flat turn ensures better control in traveling over a predefined path and avoids the fatigue that is apparent in repetitive operations like turnings.[21,22] Moreover, the heading change in a turn performed with standard rate turn (SRT), which is equal to 3 deg per second (or 180 deg turn in 1 min duration), is reliable and more predictable.[23] As a consequence, between two given points in air that requires a heading change for a level flight, instead of a shorter curvilinear path with higher turn rate, a longer path of small curvature with turning rate less than that of the SRT is generally practiced.[22,23] According to Altair Virtual Airlines,[23] the rule of thumb is to perform an SRT with bank angle less than one half of the change in the heading. For a 30/30 procedure turn, Read and Graham[11] mention a maximum allowable change in heading angle by 30 deg. Therefore, in order to change the heading by 30 deg, maximum bank angle should be limited to 15 deg. Further, if the bank angle reaches its maximum value of 15 deg, it should be maintained at 15 deg to follow a circular level turn. Finally, the aircraft should start coming back to the level flight when there remains a heading difference equal to the maximum bank angle (15 deg in this case). This arrangement ensures a turn rate less than SRT. Similarly, 1/2 SRT turn is formulated with thumb rules by aviation authorities.[24]

Considering the practical experience and preference of flying crew and the complexity of iterative solution for solving the spiral-based equations, an approximate model is developed in this paper for the calculation of the length of the trajectory from point A to C and then from C to D by simplifying the possible geometric arrangement. According to this arrangement, the length of travel over the modeled trajectory of aircraft in curvilinear path from point A to C and in 180-deg level turn from point C to D are connected at point C with zero banking angle.

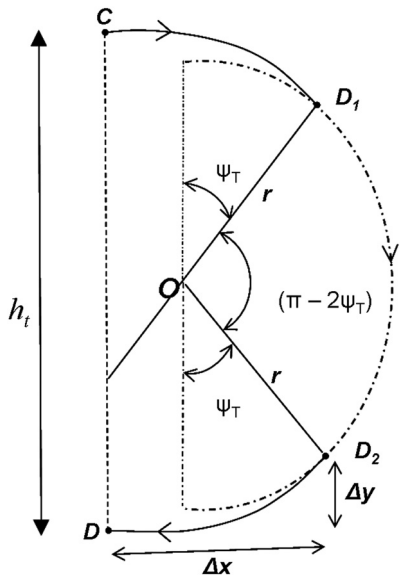

Fig. 2 Schematic view of circular trajectory and transition curves of flight path.

As a result, maintaining the continuity of curve with zero bank angles at point C, these curves can be formulated separately. The mathematical expressions for transition curves and circular curves are based on the same calculation steps. First, the calculation steps are shown for the 180-deg level turn from point C to point D and later similar steps are adopted for approximating the curvilinear path from point A to C.

3.1 *Modeling of 180-deg Level Turn*

Zdanovich[25] describes a heuristic method and formulation for modeling a turn described by circular arc that is adjoined by transition curves at the ends and changes the heading of aircraft by a specific angle in a level turn.

Figure 2 shows the turning geometry of a 180-deg level turn on consecutive flight lines. An aircraft enters at point C on a transition curve with zero bank angle, joins the circular curve at D_1, and travels over it to D_2 with maximum banking angle (β_m) and finally exits with transition curve at D. Ideally, point D should match with the right end coordinates of the $(i+1)$'th strip. Therefore, modeling the geometry of circular curve should be initiated with point C. Coordinates of point C can be obtained by projecting the geometry of the lower half of curves utilizing the property of symmetry. Angle ψ can be calculated using the coordinates of points A and C. If angle ψ turns out to be more than the maximum allowable change in the heading angle (ψ_{Max}), the curve for turn from point C to D should be shifted rightward by the required distance so as to limit ψ up to ψ_{Max}.

Zdanovich[25] assumes a constant rate of banking ($\dot{\beta}$) and consequently evaluates the transition period (T_m) to attain maximum bank angle (β_m) as linear and nonlinear functions of time, respectively. During the transition period (T_m), an aircraft is banked (rolled in) to the maximum bank angle (β_m). The maximum value of heading change (ψ_T) and the change along X and Y coordinate axes to reach the end point of a transition curve, where circular curve commences, are given by

$$T_m = \left(\frac{\beta_m}{\dot{\beta}}\right), \tag{1}$$

$$\psi_T = \left(\frac{VT_m}{2r}\right) \approx \left(\frac{gT_m\beta_m}{2V}\right), \tag{2}$$

$$\Delta X = VT_m, \tag{3}$$

$$\Delta Y = \frac{gT_m^2\beta_m}{6}. \tag{4}$$

Radius of a circular level turn with given aircraft speed and banking angle (β_m) is provided by[7,8]

$$r = \left(\frac{V^2}{g \tan \beta_m}\right). \tag{5}$$

Coordinates of point $C(X_C, Y_C)$, point $D(X_D, Y_D)$, center point (X_0, Y_0) of the circular portion and horizontal distance (h_t) between points C and D can be written as

$$X_C = X_{i+1}^R + Vt_c, \tag{6}$$

$$Y_C = Y_{i+1} + 2(\Delta Y) + 2(r \cos \psi_T), \tag{7}$$

$$X_D = X_{i+1}^R + Vt_c, \tag{8}$$

$$Y_D = Y_{i+1}, \tag{9}$$

$$X_0 = X_D + \Delta X - r \sin \psi_T, \tag{10}$$

$$Y_0 = Y_D + \Delta Y + r \cos \psi_T, \tag{11}$$

$$h_t = 2(\Delta Y + r \cos \psi_T). \tag{12}$$

The length of traveling path along the curve from point C to D can be written as

$$L_c = 2VT_m + (\pi - 2\psi_T)r. \tag{13}$$

As Zdanovich[25] considers the banking of 30 deg in 3 s duration with constant rate, the rate of banking ($\dot{\beta}$) can be calculated as 10 deg per second. Therefore, for the maximum banking of 25 deg, the transition period T_m is equal to 2.5 s. Table 1 below shows the values of various variables, namely, r, ΔX, ΔY, ψ_T, L_c, and h_t for a range of speed values.

The value of transition period T_m is 2.5 s, which is too small. However, it is evident from Table 1 that ignoring the transition period by assuming it to be zero will make the values of ΔX and ΔY zero and lead to erroneous calculations of h_t and coordinates of points C and D, which are important for preparing the flight plan.

3.2 *Modeling of Curvilinear Path from Point A to Point C*

Figure 3 shows a possible mechanism of maneuvering of the aircraft in the trajectory from point A to C for a consecutive turn. This figure illustrates clearly the different components of travel, i.e., an arrangement of possible curvilinear paths and straights.

Table 1 Calculations of variables of 180-deg level turn.

V (m/s)	r (m)	ψ_T (deg)	ΔX (m)	ΔY (m)	h_t (m)	L_c (m)
45	442.67	7.281	112.50	4.46	887.13	1503.20
50	546.51	6.552	125.00	4.46	1094.80	1841.91
55	661.28	5.957	137.50	4.46	1324.33	2214.96
60	786.98	5.460	150.00	4.46	1575.73	2622.35
65	923.60	5.040	162.50	4.46	1848.98	3064.08
70	1071.16	4.680	175.00	4.46	2144.09	3540.15
75	1229.65	4.368	187.50	4.46	2461.07	4050.55

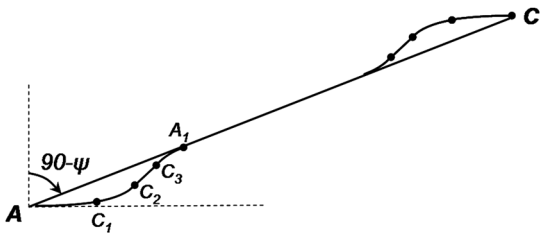

Fig. 3 Schematic view of conceptualization of flight path from point A to point C.

In order to change the heading of an aircraft by an angle ψ over the length L_1 of the straight line from point A to point C, the travel length from point A to point C is illustrated as curvilinear path formed by two curves and a straight line connecting these curves. Curve $AC_1C_2A_1$ is shown originating at point A and another curve, which is similar to $AC_1C_2A_1$, is shown ending at point C. The aircraft from zero banking angle at point A, by travelling along the transition curve AC_1, gradually reaches to bank angle (β_1) in time period T_1 and changes its heading by angle ψ_1. At the end of the transition curve at point C_1, the aircraft moves along circular arc C_1C_2 with a constant bank angle (β_1). At point C_2, the aircraft starts traveling over transition curve C_2A_1 and reaches point A_1 with zero banking angle in time T_1. After the desired change in heading (ψ), at point A_1, the aircraft starts traveling along the straight line. After traveling over the straight line, the aircraft again follows the curve, which is similar to $AC_1C_2A_1$, and reaches to point C with zero value of banking angle. In the process of traveling over the transition curves, circular arcs, and the straight line from point A to point C, the aircraft changes its heading angle by ψ. In some cases, it is possible that the length of the straight line in the curvilinear path may be zero and the curvilinear path consists of only two similar and connected curves.

The change in heading angle ψ from point A to C is measured positive in the direction away from the next strip. Moreover, as stated earlier, the change in the heading angle (ψ) is decided by calculation subjected to its maximum allowable value (ψ_{Max}). Hereafter, as explained earlier with calculations, the aircraft enters through a transition curve into a circular curve from point C and exits also through a transition curve and reaches point D.

The travel length from point A to point C comprises four transition curves, two circular curves and one straight line segment. However, the calculation of the length of travel for six curves and a straight line is complicated and cumbersome. The complicated calculations are avoided by adopting a simplified model suggested by Walker.[26] As shown in Fig. 4, the model approximates the length of travel from point A to point C by an S curve or two inverted but connected circular curves. The S curve is appended with two transition curves at the ends (i.e., at points A and C) for better estimate of the turning time. The transition curves are assumed to occur only at point A and point C, and all other transition curves and straight lines, which may occur intermittently, are assumed to be included in the circular arcs, as shown in Fig. 4. The proposed model of two circular curves with transition curves at the ends provides a slight overestimate of travel length. However, it avoids the cumbersome calculations by avoiding the connected intermediate transition curves and straight line segment.

Based on this simple and approximate model, which consists of two circular arcs, the maximum allowable change in heading angle at point A (ψ_{Max}) can be estimated. The angle ψ_{Max} confirms the geometric arrangement of consecutive turn by ensuring the compatibility and connectivity at point C between the curvilinear path from point A to C and 180-deg level turn from point C to D. In order to change the angle formed by an S turn by a value equal to two times of ξ, the minimum length of a straight line from point A to point C should be equal to

$$L_0 = 4r_1 \sin\left(\frac{\xi}{2}\right). \tag{14}$$

Walker[26] provides the mathematical expression to estimate the angle ξ. The modified expression according to the width of the 180-deg level turn (h_t) and effective swath (B) is written as

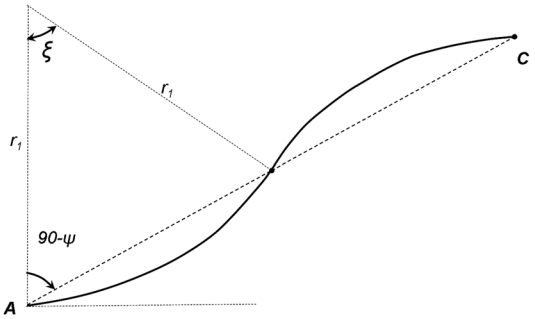

Fig. 4 Schematic view of modeled flight path (after Walker[26]).

$$\cos \xi = \left[\frac{2r_1 - (h_t - B)}{2r_1}\right], \tag{15}$$

where $r_1 = V/\dot{\psi}_{\text{Max}}$ = radius of a circular arc of curvilinear path from point A to point C. $\dot{\psi}_{\text{Max}}$ = maximum allowable rate of turn on a circular path, i.e., maximum angular speed.

Substituting the value of ξ from Eq. (15) to Eq. (14) gives

$$L_0 = \sqrt{\frac{8V(h_t - B)}{\dot{\psi}_{\text{Max}}}}. \tag{16}$$

The available length (L_1) of straight line between points A and C is calculated by considering the width of 180-deg level turn (h_t) and effective swath (B) as

$$L_1 = \left(\frac{h_t - B}{\sin \psi}\right). \tag{17}$$

Coordinates of the ends of the consecutive flight lines are not considered as these may calculate a smaller value of angle ψ. As explained earlier, a pilot always prefers to travel by standard rate of turning (SRT) or less; the available length (L_1) should be at least equal to or more than the minimum length (i.e., $L_1 \geq L_0$). Therefore, the following inequality restricts the maximum value of angle ψ as

$$\psi_{\text{Max}} \leq \sin^{-1}\left[\sqrt{\left(\frac{h_t - B}{8V}\right)\dot{\psi}_{\text{Max}}}\right]. \tag{18}$$

Equation (18), which limits the value of angle ψ, is a function of speed of the aircraft, width of 180-deg level turn, effective swath (or spacing between adjacent flight lines), and the rate of turning. Taking SRT (rate of turn $\leq$3 deg per second) as the maximum rate of turning, curves showing the values of maximum allowable change in heading angle (ψ_{Max}) against the speed (V) are drawn for different values of effective swath (B) in Fig. 5. The speed is selected in the range of 40 to 77 m/s (~80 to 150 knots). The values of the effective swath are 30, 130, 230, 330, 430, and 530 m, which cover a wide range of the possible values from minimum to maximum.

In the calculation process for ψ_{Max}, the value of radius of turn of circular arc (r_1) is calculated according to the maximum rate of turning ($\dot{\psi}_{\text{Max}}$). However, for another value of angle ψ, which is less than ψ_{Max}, the rate of turning ($\dot{\psi}$) will also be less than the SRT as shown by Eq. (19).

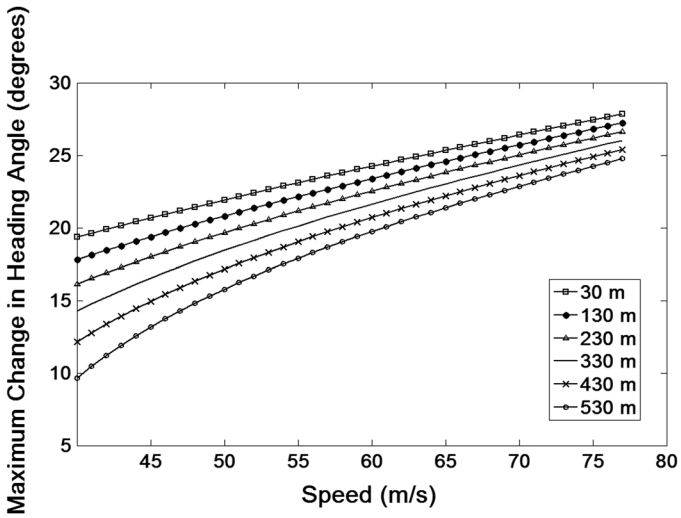

Fig. 5 Maximum allowable change in heading angle at point *A*.

$$\dot{\psi} = \left(\frac{8V\sin^2\psi}{h_t - B}\right). \tag{19}$$

With the calculated value of $\dot{\psi}$, the radius of circular arc (r_1), bank angle at the end of the transition curve (β_1), time required for the transition (T_1 or transition period), and the change in the heading during transition period (ψ_1) can be calculated as[25]

$$r_1 = \left(\frac{V}{\dot{\psi}}\right), \tag{20}$$

$$\beta_1 = \tan^{-1}\left(\frac{V\dot{\psi}}{g}\right), \tag{21}$$

$$T_1 = \left(\frac{\beta_1}{\dot{\beta}}\right), \tag{22}$$

$$\psi_1 = \left(\frac{VT_1}{2r_1}\right) \approx \left(\frac{gT_1\beta_1}{2V}\right). \tag{23}$$

In the above equations, $\dot{\psi}$ is the rate of turn and $\dot{\beta}$ is the rate of banking angle during transition period. The value of rate of turn for SRT is 3 deg per second. The change in heading angle during the transition period is expressed by Eq. (23). If the change in angle between the aircraft position after transition period (T_1) and point A is more than total heading change (ψ) from A to C, it conveys that the transition curve is not required as the circular curve is extremely flat. An extremely flat curve can be considered as a single circular arc of small curvature (or straight line). Owing to the small discrepancy raised due to the mismatch between the circular arc length and actual length of the trajectory, transition period (T_1) is added. Therefore, the length of the curvilinear path from point A to point C is calculated in two cases as

$$L' = L_1; \quad \text{if } (\psi_0 > \psi) \quad L' = 2VT_1 + 4r_1\sin^{-1}\left(\frac{L_1}{4r_1}\right); \quad \text{if } (\psi_0 \le \psi), \tag{24}$$

where ψ_0 is the slope of the line joining the point A and position of aircraft after the transition period T_1 and is given by

$$\psi_0 = \tan^{-1}\left(\frac{gT_1\beta_1}{6V}\right). \tag{25}$$

Prior to performing the calculations for turning time, the X coordinates of the end of the upcoming lines are modified by the term Vt_c. Therefore, the sum of the lengths provided by Eqs. (13) and (24), when added to difference of modified X coordinates of consecutive flight lines (δX) and the term Vt_c, which represents equivalent distance of cushion period for the given speed, will provide the total distance (L_T) covered in a consecutive turn as

$$L_T = L_c + L' + \delta X + Vt_c. \tag{26}$$

3.3 *Modeling of U-Turn*

Case-2 ($B \ge h_t$): This is a U-turn, i.e., two 90-deg turns joined by a straight line. These two turns, each performing a change in direction by 90 deg, require two pairs of transition curves. Each pair of transition curve provides time to achieve the maximum banking at the beginning of circular curve and zero banking after completing the circular curve. In this case, the minimum horizontal distance between point C and point D and travel length should be

$$h_t' = 2[\Delta Y + \Delta X + r(\cos\psi_T - \sin\psi_T)], \tag{27}$$

$$L_c = 4VT_m + 2r\left(\frac{\pi}{2} - 2\psi_T\right). \tag{28}$$

As shown in Fig. 2, for maintaining a constant bank angle on circular path from point D_1 to point D_2, the desired horizontal distance between point C and point D and travel length are given by Eqs. (27) and (28), respectively. There may be a conflicting situation where the available distance between point C and point D is higher than h_t and smaller than h_t'. In such intermediate situations, though pilot can skillfully maneuver using navigational aids for an ignored short distance and reach the destination point successfully, the estimation of correct time is critical. Transition curves at the end of the first circular turn and the start of the second circular turn between point C and point D cover the angular distance of $2\psi_T$. It can be shown by a numerical example again that assuming a circular path for the angle of $2\psi_T$, a distance equal to $2(\Delta X)$ in a turn will underestimate the time duration approximately by an amount equal to the transition period (T_m). As shown in Table 1 and discussed earlier, for banking by maximum bank angle of 25 deg at the banking rate of 10 deg per second, the demand for a change in X and Y coordinates (ΔX,ΔY) is considerable and may lead to erroneous estimate of coordinates. Therefore, though it is possible to estimate the correct time by applying the correction to transition period, it is not advised as the aircraft is not guaranteed to reach the consecutive flight line. For example, the horizontal offset ($=2\Delta X + 2\Delta Y$) is equal to 259 m for a speed of 50 m/s. Another possible solution is to reduce the bank angle, which will reduce both angle ψ_T and the transition period (T_m), while increasing the radius of circular turn (r). Increased radius of the turn for circular portion will certainly increase the travel length and consequently the travel time, but will ensure a correct reach to the destination. Equating the radius of the turn to half of the swath is a good approximate criterion and will obtain the new value of bank angle (β_m'). Recalculations for transition period (T_m), angle ψ_T, radius of turn (r), and the travel length (L_c) using Eqs. (1), (2), (5), and (13) are imperative. New angle of bank (β_m') is given by

$$\beta_m' = \tan^{-1}\left(\frac{2V^2}{Bg}\right). \tag{29}$$

For a speed of 50 m/s, banking by maximum bank angle of 25 deg and banking rate of 10 deg per second eventually calculates the values of h_t and h_t', respectively, as 1094.8 and 1220.07 m. With varying values of the effective swath between h_t and h_t', Table 2 shows the new value of bank angle (β_m') and recalculated values of transition period (T_m), radius of turn (r), change in heading angle (ψ_T), change in X and Y coordinates $(\Delta X, \Delta Y)$, width of 180-deg level turn (h_t), and the length of curve (L_c).

It is evident from Table 2 that the approximate formula for calculating β_m' from Eq. (29) estimates h_t (after modification) in close agreement with h_t' (before modification). Moreover, any numerical difference between the two variables is so small that the resulting misalignment can be corrected during the cushion period. Similar calculations for the other values of speed and effective swath can also be performed using the approximations suggested above and the length of the turn can be calculated by Eq. (26).

Table 2 Calculations of variables of U-turn when $h_t < B < h_t'$.

B (m)	β_m' (deg)	r (m)	ψ_T (deg)	ΔX (m)	ΔY (m)	h_t (m)	L_c (m)
1119.80	24.473	559.90	6.261	122.36	4.18	1121.48	1881.34
1144.80	23.999	572.40	6.006	120.00	3.94	1146.40	1918.24
1169.80	23.543	584.90	5.766	117.71	3.72	1171.33	1955.23
1194.80	23.102	597.40	5.539	115.51	3.52	1196.26	1992.30
1219.80	22.677	609.90	5.326	113.39	3.33	1221.19	2029.44

4 Modeling of Nonconsecutive Turn

When an aircraft, after negotiating a flight line, turns and reaches a flight line which is not juxtaposed, the turn is called nonconsecutive (as shown in Fig. 6). In this case, the aircraft turns naturally according to the banking angle and turning radius in a constant direction (clockwise or anticlockwise). A clockwise turn at the end of a forward direction flight will take an aircraft from a lower number flight line to a higher number flight line. This type of turn, in view of the increase in the number of flight line, is called a forward turn. Similarly, a clockwise turn at the end of a reverse direction flight line will take an aircraft from a higher number flight line to a lower number flight line. As this turn is taking an aircraft from a higher flight number to a lower flight number, it is called a reverse turn. The same, as in the above, will be true if the term clockwise is replaced by anticlockwise and forward by reverse. In a forward turn, two flight lines, which are covered by an aircraft in sequence, are separated by a specific integer number of lines that creates an interval of lines or the line interval. Similarly, another value of line interval is required for performing a reverse turn. As a result, the line intervals for reverse and forward turns are different. The spacing for reverse turn is less by one line than that of the forward turn. Figure 6 shows the NCT over a rectangular AOI. As turning is performed in a systematically smooth and natural way along a constant direction (say clockwise and counterclockwise), the NCTs are also called constant direction turns (CDT).[11]

As shown in Fig. 6, there are 19 flight lines. The flight lines on AOI are indicated by dashed lines with arrows, which show the flight direction over flight strips on map. Upper and lower ends of the vertical flight lines are similar to the right and left ends of horizontal flight lines, respectively. The aerial survey commences from point *S* and ends at point E. However, the turning starts from the upper end of the extreme left line (first line) to the next line in a clockwise direction with respect to the nose of the aircraft or the viewing direction of pilot. As a result, at the end of the 1st flight line, the aircraft takes a long forward turn to the 6th flight line. Further, at the end of the 6th flight line, the aircraft performs a short reverse turn to the 2nd numbered flight line. Therefore, a pair of long clockwise forward turn and a short clockwise reverse turn is formed by forward and reverse turnings, respectively. Accordingly, the aircraft covers first ten flight lines of AOI in the similar manner of forward long turn and reverse short turn in a clockwise direction. After traveling over the 10th flight line, i.e., once all preceding flight strips are covered, the aircraft starts traveling in a counterclock wise direction (or left-handed direction) to fly over the remaining flight lines in a similar fashion till the end of the survey operation at point *E*.

Ordering of the flying operations for turning can be represented by direction of flight path over the flight lines and flight line numbers. If an aircraft travels over a flight line in the vertically upward direction along the longer dimension of this page, the direction of the flight path over that flight line is written as fore (or F). Conversely, when the aircraft travels vertically downward, the direction of the flight path over that flight line is written as rear (or R). Therefore, for the configuration of nonconsecutive turns with clockwise and anticlockwise turning, the lines

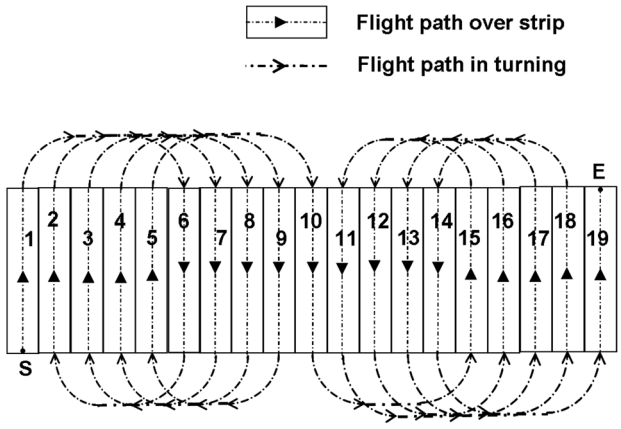

Fig. 6 Schematic view of nonconsecutive turns over rectangular area of interest (AOI).

covered, appearing in specific order as shown in Fig. 6, are represented as 1F-6R-2F-7R-3F-8R-4F-9R-5F-10R-15F-11R-16F-12R-17F-13R-18F-14R-19F. It should be noted that this sequence is a valid expression with an assumption that flying starts at point S in a predefined flying direction, which is upward on this page. With this terminology, any nomenclature for turns (e.g., long and short or forward and reverse) does not depend upon the ordering or sequencing of flight lines representing the flying operations. However, for the purpose of better and easier explanations, these terms are used in the forthcoming discussion for deriving the algorithm that calculates the flight duration.

The nonconsecutive turning mechanism, as can be seen in Fig. 6, is a set of forward long turns and reverse short turns in a constant direction between the flight lines. The line interval, i.e., the separation between flight lines between which a short or long turn is taken, can have different values. However, minimizing the line interval, i.e., taking the turn at the earliest opportunity, will ensure minimum time taken for these turns.

The line interval is the number of flight lines within which a turn is realized. The distance for minimum line interval can be decided by minimum travel length (h_t') [expressed by Eq. (27)]. The line interval for a long turn requires one additional line. For a given spacing (effective swath) of flight strips, the travel length of a long turn or short turn is equivalent to the travel length in case of a consecutive turn with swath width being more than the minimum distance (h_t') required for consecutive turning. Each long and short turn has a constant travel length for turning except for the length caused by the difference in the coordinates of the end of strips that are joined by the turns. Therefore, the line interval for a forward turn (l_f) and a reverse turn (l_r) can be calculated as

$$l_f = \text{ceiling}\left(\frac{h_t'}{B}\right) + 1, \tag{30}$$

$$l_r = l_f - 1. \tag{31}$$

Turning by a long turn from i'th strip to j'th strip requires a line interval of l_f number of lines. The line number of j'th strip can be written as

$$j = i + l_f. \tag{32}$$

As indicated earlier, the coordinates of the right end and left end of a flight strip are increased and decreased, respectively, by a distance that is necessary for creating the cushion time (i.e., Vt_c). A short turn will be created by turning from j'th strip to $(i+1)$'th strip. The turning lengths for a long turn (L_f) and a short turn (L_r) can be determined as

$$L_f = 4VT_m + 2r\left(\frac{\pi}{2} - 2\psi_T\right) + B(l_f) - h_t' + Vt_c, \tag{33}$$

$$L_r = 4VT_m + 2r\left(\frac{\pi}{2} - 2\psi_T\right) + B(l_f - 1) - h_t' + Vt_c. \tag{34}$$

As explained earlier for the consecutive turn, the term δX representing the difference of coordinates, should be added to calculate the total length of the turn between the two specific flight lines. However, it is not explicitly mentioned in the expressions of NCT.

4.1 *Algorithm for Turning Time for Nonconsecutive Turning*

After deciding the line interval, turn length, source line, and destination line, the mechanism of nonconsecutive turning can be modeled using an algorithm. According to the algorithm, an aircraft traveling over any flight strip preferably takes a reverse turn with a short turn provided the destination flight line exists and is not yet covered. However, if the short reverse turn is not

possible to perform, a long forward turn is performed. This process is repeated till all the flight strips are covered. This algorithm can be explained by Fig. 6. In Fig. 6, a total of 19 flight lines are shown. After covering the 1st flight line, the aircraft takes a forward turn to the 6th flight line by a long turn as it is not possible to form a short reverse turn. At the end of the 6th flight line, the aircraft turns to 2nd flight line by a short reverse turn because the 2nd flight line exists and is not covered yet. This continues till 1st to 10th flight lines are traveled by a series of long and short turns in clockwise direction. After reaching the 10th flight line from the 5th flight line by a long forward turn, it is imperative that the aircraft should turn by a short turn in reverse direction. However, as all preceding flight lines have already been covered, the aircraft rather takes a long forward turn to the 15th flight line in counterclockwise direction. In the above process of nonconsecutive turning, the line interval for long turn and short turn are 5 and 4, respectively. At this stage, the aircraft repeats the same steps by a series of short reverse turns and long forward turns to cover the rest of the AOI. This continues till all the flight lines are exhausted.

4.2 *Algorithm for Estimating Turning Time of Variants of Nonconsecutive Turn*

In the process of turning as shown above, a situation may arise, as shown in Fig. 7, when turning in forward direction or in reverse direction is not possible because the destination flight lines, both for long and short turns, are already covered or unavailable. However, there are some more flight strips, which are still not covered. There are two methods of covering the remaining flight strips: natural nonconsecutive turning (NNCT) and hybrid nonconsecutive turning (HNCT).

The complete arrangement of turning, since the beginning of the survey from point *S* to the end point *E* in Fig. 8, is termed as NNCT. More specifically, this turning mechanism is named here as natural nonconsecutive turning of second type (or NNCT-2). The natural nonconsecutive turning of first type (NNCT-1) will be explained later. Turning by NNCT-2 mechanism comprises a series of long and short turns (as shown in Fig. 7). As is evident from Fig. 8, each of the remaining flight lines is covered by performing a set of long turn and short turn outside the AOI.

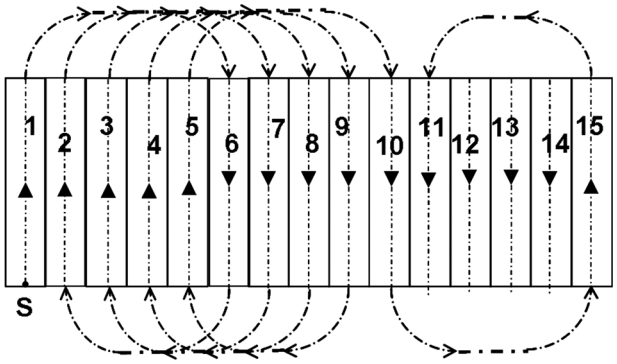

Fig. 7 Schematic view of incomplete nonconsecutive turns over rectangular AOI.

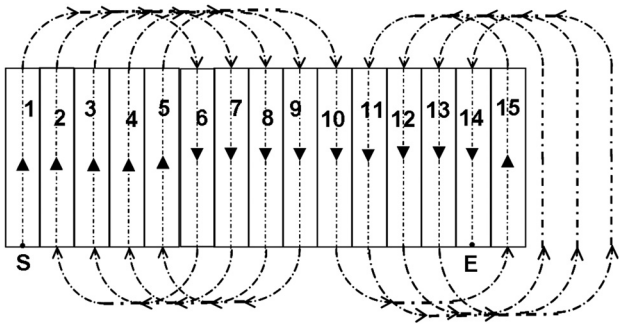

Fig. 8 Schematic view of natural nonconsecutive turning with extra turns (type-2 or NNCT-2).

The long turn, short turn, and the extra flight lines together are addressed as an extra turn. It can be observed that unlike a set of long turn and short turn that covers two flight lines in the AOI, an extra turn can only cover one flight line as the extra turn lies outside the AOI.

An extra turn essentially consists of a pair of long turn and short turn with cushion times and an additional flight line outside the AOI. The length of additional flight line, which lies outside the AOI, varies according to values of X coordinates of opposite ends of two consecutive flight lines. However, in each extra turn, travel length for a pair of long turn and short turn with a distance equivalent to the cushion time is a constant. The constant travel length in an extra turn is given by

$$L_e = 8VT_m + 4r\left(\frac{\pi}{2} - 2\psi_T\right) + B(2l_f - 1) - 2h_t' + Vt_C. \tag{35}$$

While performing an NNCT-2 turn, a special case may occur where there is a further possibility of minimizing the length of travel. In other words, in order to achieve the economy in flight duration, it is imperative to search a possibility of forming a short forward turn. Such a case is illustrated by Fig. 9. Instead of performing an extra turn (by NNCT-2), i.e., covering one flight line lying inside and other outside the AOI, a better solution is to cover both flight lines inside the AOI. This turning mechanism is termed as NNCT-1. In this turning mechanism, long and short turns are performed in such a way that while one of the remaining flight lines of AOI is covered by one flight path, the other flight path lies over the already covered flight line on the AOI. As shown in Fig. 9, instead of initiating the extra turn by a long turn for the remaining flight lines, a short turn is performed. The short turn repeats the flight line as the aircraft covers a flight line that is already covered. After this short turn, a set of long turn and short turns are traveled to cover the remaining flight lines in successive manner. NNCT-1 mechanism results in a few strips being covered twice as shown in Fig. 9. Turning with NNCT-1, which is applicable under certain circumstances, certainly reduces the time duration compared to NNCT-2. It should be noted that while it is possible to perform turning by NNCT-2 mechanism, NNCT-1 is more economical. In Fig. 9, for a better explanation of NNCT-1 mechanism, some of the long and short turns are drawn with different lengths and shapes.

The NNCT mechanism also suggests that instead of turning by NNCT-1 or NNCT-2 mechanism, consecutive turning can be performed for the remaining flight strips. However, as the nonconsecutive turning is desired only when consecutive turning is difficult to perform, the possibility of hybridizing the nonconsecutive and consecutive turnings in one mission is preferably not adopted in field practices.[3] Considering the possible economy in the flight operations and depending upon the choice of a pilot, there is a slight possibility to perform HNCT. Like NNCT, HNCT can also be imagined of two types: HNCT-1 and HNCT-2.

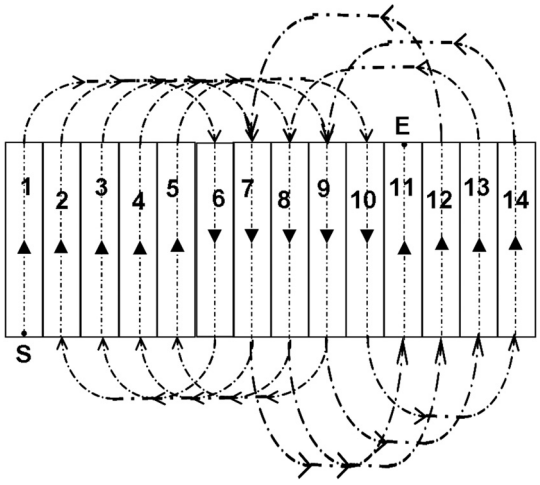

Fig. 9 Schematic view of natural nonconsecutive turning of type-1 (NNCT-1).

5 Algorithm for Evaluating Optimal Turning Mechanism

A comprehensive and automated flight planning system for LiDAR and photographic data acquisition should consider all variables, like speed, overlap, flying height, FOV, and flying direction, which in turn determine the length of the flight lines and width of strips, line spacing, and configuration of longer and shorter flight lines, as essential features and elements.[27] However, considering the limited scope of this paper on turning mechanisms, the described algorithm presents a decision-making process for the selection of an optimal turning mechanism.

Due to various turning mechanisms, namely consecutive, nonconsecutive, and hybrid, a decision-making process is required for selection of the turning mechanism, which corresponds to the minimum turning time. The decision-making process is complicated due to the variants of the above mentioned nonconsecutive turning mechanisms (e.g., NNCT-1, NNCT-2, HNCT-1, and HNCT-2 mechanisms). The following flight planning algorithm summarizes the decision-making process for the selection of the right turning mechanism. It is assumed that speed, overlap, flying height, FOV, and flying direction are given.

Calculate:

Consecutive Turning Time:

Calculate: Turning time for consecutive turning mechanism

Nonconsecutive Turning:

Check: Possibility for NNCT-1
Calculate: Turning time for NNCT-2 and NNCT-1 (if exists)

Hybrid Turning:

Check: Possibility for HNCT-1
Calculate: Turning time for HNCT-2 and HNCT-1 (if exists)

Decision Making:

Calculate: Minimum turning time among the times contributed by all mechanisms (consecutive, NNCT-1, NNCT-2, HNCT-1, and HNCT-2)
Select: Turning mechanism corresponding to minimum turning time

The flight planning algorithm written above calculates the minimum turning time and the corresponding turning mechanism. In the above algorithm, hybrid nonconsecutive turning mechanisms (HNCT-1 and HNCT-2) are optional. On the other hand, a tuning mechanism should also be selected according to applications of the acquired data and physical limitations of the acquisition system. For example, orthophoto production using aerial photographs demands minimum variation in sun illumination over adjacent images captured over two neighboring flight lines. Therefore, if significant variation in the sun light illumination is expected over the AOI during a mission of photographic data acquisition, consecutive turning mechanism should be preferred.

6 Conclusion and Future Work

Turning of an aircraft in an aerial survey to switch between two flight lines, can be performed by consecutive and nonconsecutive turning mechanisms. Instead of adopting iterative and complicated mathematical models of turning or simply a constant time for turning, the turning mechanisms are developed using the available heuristic information, approximate mathematical models, and current practices adopted by pilots for turning with specific preferences for comfort, confidence, and high precision. Along with the turning on a circular trajectory of aircraft, this paper also considered the transition period. The illustrated method adjusts the travel length of the circular arc for the period of transition curves by mathematical approximations. Transition period is a function of speed and depends upon the turning rate and banking rate. During the transition period, an aircraft changes the heading angle and bank angle simultaneously to specific values such that the required trajectory to the destination point can be formed. The transition period ranges from 2 to 3 s for the frequently used values of maximum heading change and maximum bank angle. Despite being small in value, for considerable speed of the aircraft, the transition

period results in a long distance. Ignoring this long distance will accumulate errors, which may lead to misalignment of aircraft trajectory on the flight lines.

The turning time, in both consecutive and nonconsecutive turnings, is a function of cruise speed, effective swath, and maximum allowable turn rate and banking rate. The demonstrated calculations show that the period of transition from straight line to circular path results in considerable distances, which cannot be ignored. The formulated transition period and horizontal course reversal are used to develop the formulations of consecutive and nonconsecutive turning mechanisms. Unlike the consecutive turning mechanism, which is discussed in the literature, switching to the next line in nonconsecutive manner is performed by continuous rotation of aircraft in one direction (clockwise or counterclockwise) with a defined line interval. The paper proposes a strategy of turning at earliest opportunity. For the given speed, effective swath, and the number of flight lines, the formulations that calculate line interval to decide the destination flight line with respect to the current flight line in nonconsecutive turning mechanism is derived. Further, the natural and hybrid nonconsecutive turning mechanisms are suggested as variants of nonconsecutive turning mechanism. The demonstrated calculations provide numerical results for the values of relevant variables of turning mechanisms. Further, the calculations are carried out to determine the turning distance evaluated for a range of aircraft speed.

The developed system of turning can be generalized for any airborne survey performed with a rectangular swath. For the given speed and other variables, an algorithm that considers various turning mechanisms for decision making for arriving at the optimal turning mechanism is presented. The proposed algorithms have the potential to be incorporated into an optimization framework, which utilizes the GA (or EA) to minimize the total time of flight, i.e., strip time and turning time, while also satisfying the data quantity and quality requirements under the available sensor and platform constraints.

The future research should be emphasized to develop a strategy to incorporate the ordering of flight lines and turning mechanisms into the evolutionary algorithms, which can determine the turning mechanism causing minimum flight duration. Moreover, algorithms should also be flexible enough to consider the additional flying time that is contributed by dry runs, time for climb and descend of aircraft, and locations of the airports around the AOI for optimal planning of data acquisition.

Acknowledgments

Authors are thankful to Dr. Adriaan Combrink (C K Aerial Surveys, South Africa), Dr. Gary Llewellyn (NERC Airborne Research and Survey Facility, Oxford, UK), Capt. K. B. Singh (U.P. Aviation Authorities, India), Capt. Amit Dahiya (Punjab Aviation Club, India), and Dr. Jacques Populus (Department of Coastal Environment Dynamics, Applications Géomatiques, Plouzane, France) for sharing their experience and information. Comments of the reviewers helped in improvising the paper.

References

1. E. P. Baltsavias, "Airborne laser scanning: basic relations and formulas," *ISPRS J. Photogramm. Remote Sens.* **54**(2–3), 199–214 (1999), http://dx.doi.org/10.1016/S0924-2716(99)00015-5.
2. M. M. R. Mostafa and J. Hutton, "Direct positioning and orientation systems: how do they work? What is the attainable accuracy?," April 2001, http://www.applanix.com/media/downloads/articles_papers/POSAV_2001_04_DirectPositioning.pdf (23 August 2012).
3. A. Combrink, C K Aerial Surveys, South Africa, private communications (2012).
4. Federal Aviation Authorities (FAA), "Quarterly magazine of Federal Aviation Administration (FAA), USA, Issue 1," *Air Traffic Bulletin*, February 2006, http://www.faa.gov/air_traffic/publications/bulletins/media/atb_feb_06.pdf (5 July 2012).
5. P. Johnson, "Unmanned aerial vehicle as the platform for lightweight laser sensing to produce sub-meter accuracy terrain maps for less than $5/km^2$," in *CUSJ Spring Research Symposiums 2006–2008*, Columbia University, New York (2006).
6. R. Read and R. Graham, "Mission planning," Chapter 11 in *Manual of Aerial Survey: Primary Data Acquisition*, pp. 243–280, Whittles Publishing, Scotland, UK (2002).
7. M. Saarlas, *Aircraft Performance*, John Wiley & Sons, New Jersey (2007).

8. J. S. Wolper, "Turn performance of aircraft," *SIAM Rev.* **36**(3), 470–473 (1994), http://dx.doi.org/10.1137/1036102.
9. S. Mullender, "A note on steep turns and wind," 2006, http://www.diversiorum.org/sape/pilotage/Hudson/steepturns.html (15 July 2012).
10. G. C. Grigg, "Aeronautical aspects of biological aerial surveys," in *Aerial Surveys of Fauna Populations, Australian National Parks and Wildlife Service Special Publication No. 1*, pp. 63–74, Australian Government Publishing Service, Canberra, Australia (1979).
11. R. Read and R. Graham, "Operational procedures: first phase," Chapter 12 in *Manual of Aerial Survey: Primary Data Acquisition*, pp. 281–303, Whittles Publishing, Scotland, UK (2002).
12. G. Llewellyn, NERC Airborne Research and Survey Facility, Oxford, UK, private communication (2009).
13. S. Piel and J. Populus, "Recommended operating guidelines (ROG) for LiDAR surveys," 2007, http://www.searchmesh.net/PDF/GMHM3_LIDAR_ROG.pdf (15 July 2012).
14. J. Populus, "Department of Coastal Environment Dynamics (DYNECO), Applications Géomatiques," Ifremer, Plouzane, France, private communication (2011).
15. E. Benavent et al., "New heuristic algorithms for the windy rural postman problem," *Comput. Oper. Res.* **32**, 3111–3128 (2005), http://dx.doi.org/10.1016/j.cor.2004.04.007.
16. A. M. Rodrigues and S. Ferreira, "Cutting path as a rural postman problem: solutions by memetic algorithms," *Int. J. Comb. Optim. Probl. Inf.* **3**(1), 22–37 (2012).
17. R. Graham and A. Koh, "Survey flight management: tracking, GPS, mission planning," Chapter 7 in *Digital Aerial Survey: Theory and Practice*, pp. 123–141, Whittles Publishing, Scotland, UK (2002).
18. R. Dai and J. E. Cochran Jr., "Path planning for multiple unmanned aerial vehicles by parameterized cornu-spirals," in *Proc. of 2009 American Control Conference Hyatt Regency Riverfront*, pp. 2391–2396, IEEE (2009).
19. L. Techy, C. A. Woolsey, and K. A. Morgansen, "Planar path planning for flight vehicles in wind with turn rate and acceleration bounds," in *Proc. of 2010 IEEE Int. Conf. on Robotics and Automation*, pp. 3240–3245, IEEE (2010).
20. J. P. McCrae, "Sketch-based path design," MS Thesis, Graduate Department of Computer Science, University of Toronto (2008).
21. K. B. Singh, Uttar Pradesh Aviation Authorities, India, personal discussion (April 2012).
22. A. Dahiya, Flight Trainer and Pilot, Punjab Aviation Club, India, personal discussion (April 2012).
23. AVA, "Turns (Reference: FS2002 ground school text, FS9 Flying lessons), *Altair Virtual Airlines*, 2001, http://www.altairva-fs.com/training/ava_training_turns.htm (1 May 2012).
24. IP, "Navy flight manuals," http://navyflightmanuals.tpub.com/ (1 May 2012).
25. V. G. Zdanovich, Ed., "Current measurement by single floats," Chapter 1 in *Methods of Studying Ocean Currents by Aerial Survey*, pp. 8–107, Israel Program for Scientific Translations, Jerusalem, Israel (1967).
26. E. Walker, "A slide rule for the computation of precision turns in air survey navigation (The I.T.C. survey flight slide rule)," *Photogramm. Rec.* **4**(24), 489–502 (1964), http://dx.doi.org/10.1111/j.1477-9730.1964.tb00384.x.
27. A. Dashora, "Optimization system for flight planning for airborne LiDAR data acquisition," Ph.D. Dissertation, Department of Civil Engineering, Indian Institute of Technology Kanpur (2013).

Ajay Dashora received his MTech and PhD degree in geoinformatics specialization from Department of Civil Engineering, Indian Institute of Technology Kanpur, India, respectively, in years 2005 and 2013. His PhD thesis problem was addressing the problem of development of optimization system for airborne LiDAR data acquisition. Before joining the PhD program in January 2009, he worked as a research associate in the area of flood modeling, as a senior engineer in automobile industry, and as a regional data sourcing manager in navigation industry. After completing his PhD, he developed the standards of airborne LiDAR data acquisition

for India as senior project engineer at IIT Kanpur. His research interests include physical modeling, synthetic simulation, compatibility studies, integration of airborne data acquisition methods and techniques, application of remote sensing techniques, and use of evolutionary algorithms in remote sensing. He received the best research paper award from Indian Society of Remote Sensing in year 2006 for devising a better and cost effective technique for planning and collection of ground control points for historical images and photographs.

Bharat Lohani received his PhD degree from the University of Reading, Reading, UK, in LiDAR technology and environmental sciences, in 1999. He is currently an associate professor with the Indian Institute of Technology Kanpur, Kanpur, India, where he has been since 2002. He has interest in teaching and research in the domain of laser scanning-data capture, processing and application development. He has published papers in the area of extraction of channel networks, buildings from LiDAR data. He has developed model for predicting GPS-GDOP using LiDAR data and URP. He has been behind the development of LiDAR Simulator. He is currently co-chair with ISPRS WG V-2 and a fellow with the Institution of Surveyors, India.